

---

# Reimplementation of Denoising Diffusion Restoration Models

---

Jia Fu

Haoye Chen

Christian Siman-Chereches

## Abstract

In this paper, we reimplement the paper Denoising Diffusion Restoration Models (DDRM) from 2022 for image restoration tasks. DDRM innovatively takes advantage of a pre-trained denoising diffusion generative model for dealing with any restoration tasks that can be written as linear inverse problems. We test our implementation on dataset FFHQ which is used in the original paper and a new dataset ImageNet 1k. We also compare the performance (PSNR, SSIM, and KID) of our implementation with the ones of the original paper and other methods on the mentioned two datasets to check the reproducibility. Additionally, we perform experiments where the weights of the pre-trained models are different from the ones in the original paper. Our implementation has a very close performance compared to the original paper.

## 1 Introduction

In this work we have re-implemented the Denoising Diffusion Restoration Models (DDRM) paper. [1]

DDRM introduces a novel approach to image restoration using generative models. It leverages a pre-trained denoising diffusion generative model to efficiently and effectively solve linear inverse problems. By using the generative model's ability to capture the underlying distribution of images, DDRM can restore them with high fidelity and reduced artifacts. [1]

We try to recreate the results of DDRM by following their equations and algorithm and then comparing our estimated images with theirs for the deblur, super-resolution, and inpainting tasks. Furthermore, we compare our metrics and results with other related works mentioned in the paper, such as Deep Generative Prior (DGP) [2], SNIPS [3], and Regularization by Denoising (RED) [4]. Additionally, we conducted experiments by manipulating the weights of the pre-trained model in DDRM to examine its impact on the restoration results.

Through our re-implementation, we reinforce DDRM's effectiveness as a versatile and reproducible tool for image restoration. We managed to reproduce the results from the original paper and validated them by comparing the estimations on a sub-sample from ImageNet and FFHQ, thus we prove the reliability of the original implementation. This ability to efficiently and accurately restore degraded images is important for a wide range of applications, including medical imaging, surveillance, and content enhancement, as mentioned in [5, 6].

The code to our implementation is available at <https://github.com/JasonFu1998/Reimplementation-DDRM>.

## 2 Related work

The image restoration domain has had several advancements in recent years. One of them is the addition of generative modelling. Due to the ability to capture the inherent distribution of images, this method has become popular in image restoration tasks. [2]

In traditional deblurring methods we often rely on iterative optimization techniques, which can be computationally expensive and prone to artifacts. [7, 8] Generative models, on the other hand, provide a more efficient approach to deblurring. [9] Notable examples are Deep Image Prior (DIP) [10] and efficient blind denoising convolutional neural network (BDCNN). [11] In DIP, they demonstrate that the structure of a generator network alone captures substantial low-level image statistics without learning. [10] Conversely, in BDCNN, the tightly coupled relationship between noise level and the denoiser is fructified through an efficient blind denoising convolutional neural network. [11]

In comparison, for traditional super-resolution methods we often suffer from loss of detail and introduce artifacts. [12, 13, 14] With generative models remarkable success has been achieved, enabling high-quality restoration of images with minimal artifacts, as discussed in [15]. For example, in generative adversarial network for image super-resolution (SRGAN) the authors use a GAN-based SISR method which utilizes perceptual losses and a deep residual network to achieve photo-realistic image quality for high upscaling factors. [16] Also, in EDSR the authors focused on optimization through the removal of unnecessary modules in residual networks coupled with an expansion of the model size and a set of stabilized training procedures, surpassing existing super-resolution methods at the time. [17]

For inpainting, traditional methods often require user intervention or rely on heuristic approaches that may not effectively restore the corrupted segments, as pointed out in the survey in [18]. With generative models, however, it was proven to they are a powerful tool for inpainting, capable of consistently filling in missing regions while maintaining image fidelity. One example is in [19], where we have Context Encoders, inspired by auto-encoders and trained via convolutional neural networks to predict image regions from surrounding context. Another example is Contextual Attention Generative Adversarial Network (CGAN), a deep generative model-based approach that enhances inpainting by explicitly leveraging surrounding image features as references during network training. [20]

### 3 Method

In this section, we discuss the research problem, the original method of DDRM, and our implemented way. Section 3.1 briefly introduces the linear inverse problem and its relationship with generative models. Section 3.2 firstly introduces the denoising diffusion probabilistic models (DDPM) and then defines DDRM proposed by the selected paper. Section 3.3 briefly displays the detailed formulation of DDRM in a singular value decomposition (SVD) format. Section 3.4 illustrates the way to use pre-trained DDRM models instead of learning DDRM parameterized models. Finally, we discussed our implemented way in Section 3.5.

#### 3.1 Linear inverse problem and generative models

Many interesting tasks in image restoration can be cast as linear inverse problems that aim to recover the signal  $\mathbf{x} \in \mathbb{R}^n$  from measurements  $\mathbf{y} \in \mathbb{R}^m$  while the two components fulfill the following relationship:

$$\mathbf{y} = \mathbf{H}\mathbf{x} + \mathbf{z}, \quad (1)$$

where  $\mathbf{H} \in \mathbb{R}^{m \times n}$  is a known linear degradation matrix, and  $\mathbf{z} \sim \mathcal{N}(0, \sigma_y^2 \mathbf{I})$  is an i.i.d. additive Gaussian noise with known variance.

A generative model  $p_\theta$  can represent the implicit structure of  $x$ . Given  $\mathbf{y}$  and  $\mathbf{H}$ :

- posterior over the signal:  $p_\theta(\mathbf{x} | \mathbf{y}) \propto p_\theta(\mathbf{x})p(\mathbf{y} | \mathbf{x})$
- likelihood:  $p(\mathbf{y} | \mathbf{x})$  defined by Eq.(1)

#### 3.2 DDPM and DDRM as generative models

Various generative-model-based structures have been applied to recovery problems. They learn a model distribution  $p_\theta(\mathbf{x})$  that approximates a data distribution  $q(\mathbf{x})$  from samples. Diffusion models are the ones with excellent performance among them. In this subsection, we first introduce the structure and inference of DDPM. Then, we discussed DDRM's structure and inference proposed by the selected paper, which are conditional on  $\mathbf{y}$  compared to the ones of DDPM. Figure 1 compares

the difference between DDRM and DDPM via a specific linear inverse problem (Super-resolution + denoising).

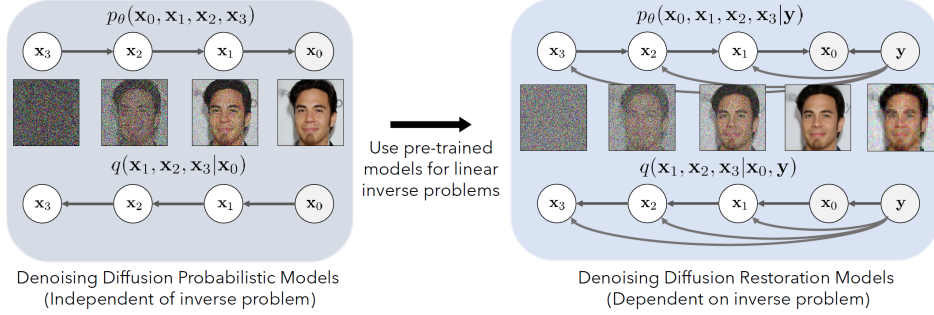


Figure 1: DDPM vs DDRM, the figure is from [1]

### 3.2.1 DDPM: structure, inference, and ELBO

Diffusion models are generative models with a Markov chain structure  $\mathbf{x}_T \rightarrow \mathbf{x}_{T-1} \rightarrow \dots \rightarrow \mathbf{x}_1 \rightarrow \mathbf{x}_0$  (where  $\mathbf{x}_t \in \mathbb{R}^n$ ), which has the following joint distribution:

$$p_\theta(\mathbf{x}_{0:T}) = p_\theta^{(T)}(\mathbf{x}_T) \prod_{t=0}^{T-1} p_\theta^{(t)}(\mathbf{x}_t | \mathbf{x}_{t+1}). \quad (2)$$

After drawing  $\mathbf{x}_{0:T}$ , only  $\mathbf{x}_0$  is kept as the sample of the generative model. To train a diffusion model, a fixed, factorized variational inference distribution is introduced based on the degradation:

$$q(\mathbf{x}_{1:T} | \mathbf{x}_0) = q^{(T)}(\mathbf{x}_T | \mathbf{x}_0) \prod_{t=0}^{T-1} q^{(t)}(\mathbf{x}_t | \mathbf{x}_{t+1}, \mathbf{x}_0), \quad (3)$$

which leads to an evidence lower bound (ELBO1) on the maximum likelihood objective [21].

### 3.2.2 DDRM: structure, inference, and ELBO

For any linear inverse problem, the selected paper defined DDRM as a Markov chain  $\mathbf{x}_T \rightarrow \mathbf{x}_{T-1} \rightarrow \dots \rightarrow \mathbf{x}_1 \rightarrow \mathbf{x}_0$  conditioned on  $\mathbf{y}$ , where

$$p_\theta(\mathbf{x}_{0:T} | \mathbf{y}) = p_\theta^{(T)}(\mathbf{x}_T | \mathbf{y}) \prod_{t=0}^{T-1} p_\theta^{(t)}(\mathbf{x}_t | \mathbf{x}_{t+1}, \mathbf{y}), \quad (4)$$

and  $\mathbf{x}_0$  is the final diffusion output. To perform inference, the authors consider the following factorized variational distribution conditioned on  $\mathbf{y}$ :

$$q(\mathbf{x}_{1:T} | \mathbf{x}_0, \mathbf{y}) = q^{(T)}(\mathbf{x}_T | \mathbf{x}_0, \mathbf{y}) \prod_{t=0}^{T-1} q^{(t)}(\mathbf{x}_t | \mathbf{x}_{t+1}, \mathbf{x}_0, \mathbf{y}), \quad (5)$$

The detailed formulations of the variation distribution depend on the degradation,  $\mathbf{H}$  in the case of problem Eq.(1) specifically.

Eq.(4) and (5) lead to another evidence lower bound (ELBO2) objective for diffusion models conditioned on  $\mathbf{y}$  (see details in Appendix A of [1]).

### 3.3 SVD-based Diffusion Process for Image Restoration

This subsection discusses the detailed formulations of Eq.(4) and (5) given known  $\mathbf{H}$ .

The selected paper considered an SVD of  $\mathbf{H}$  according to SNIPS [3] and derived Eq.(5) (the factorized variational distribution conditioned on  $\mathbf{y}$ ) based on this decomposition. The SVD of  $\mathbf{H}$  can be written as:

$$\mathbf{H} = \mathbf{U}\Sigma\mathbf{V}^\top, \quad (6)$$

$\mathbf{U} \in \mathbb{R}^{m \times m}$ ,  $\mathbf{V} \in \mathbb{R}^{n \times n}$  are orthogonal matrices, and  $\Sigma \in \mathbb{R}^{m \times n}$  is a rectangular diagonal matrix containing the singular values:  $s_1 \geq s_2 \geq \dots \geq s_m$  of  $\mathbf{H}$ , ordered descendingly.  $s_i = 0$  for  $i \in [m+1, n]$ .

The SVD of  $\mathbf{H}$  enables DDRM to perform diffusion for image restoration in its spectral space. For simplicity, we directly display the constructed formulation of the variational inference in the SVD-based diffusion process. We refer the interested reader to the selected paper [1] and [3] for more details.

" For each index  $i$  in  $\bar{\mathbf{x}}_t$ , the variational distribution is:

$$q^{(T)}(\bar{\mathbf{x}}_T^{(i)} | \mathbf{x}_0, \mathbf{y}) = \begin{cases} \mathcal{N}\left(\bar{\mathbf{y}}^{(i)}, \sigma_T^2 - \frac{\sigma_{\mathbf{y}}^2}{s_i^2}\right) & \text{if } s_i > 0 \\ \mathcal{N}\left(\bar{\mathbf{x}}_0^{(i)}, \sigma_T^2\right) & \text{if } s_i = 0 \end{cases} \quad (7)$$

$$q^{(t)}(\bar{\mathbf{x}}_t^{(i)} | \mathbf{x}_{t+1}, \mathbf{x}_0, \mathbf{y}) = \begin{cases} \mathcal{N}\left(\bar{\mathbf{x}}_0^{(i)} + \sqrt{1 - \eta^2} \sigma_t \frac{\bar{\mathbf{x}}_{t+1}^{(i)} - \bar{\mathbf{x}}_0^{(i)}}{\sigma_{t+1}}, \eta^2 \sigma_t^2\right) & \text{if } s_i = 0 \\ \mathcal{N}\left(\bar{\mathbf{x}}_0^{(i)} + \sqrt{1 - \eta^2} \sigma_t \frac{\bar{\mathbf{y}}^{(i)} - \bar{\mathbf{x}}_0^{(i)}}{\sigma_{\mathbf{y}}/s_i}, \eta^2 \sigma_t^2\right) & \text{if } \sigma_t < \frac{\sigma_{\mathbf{y}}}{s_i} \\ \mathcal{N}\left((1 - \eta_b) \bar{\mathbf{x}}_0^{(i)} + \eta_b \bar{\mathbf{y}}^{(i)}, \sigma_t^2 - \frac{\sigma_{\mathbf{y}}^2}{s_i^2} \eta_b^2\right) & \text{if } \sigma_t \geq \frac{\sigma_{\mathbf{y}}}{s_i} \end{cases}$$

where  $\bar{\mathbf{x}}_t^{(i)}$  is the  $i$ -th index of the vector  $\bar{\mathbf{x}}_t = \mathbf{V}^\top \mathbf{x}_t$ , and  $\bar{\mathbf{y}}^{(i)}$  is the  $i$ -th index of the vector  $\bar{\mathbf{y}} = \Sigma^\dagger \mathbf{U}^\top \mathbf{y}$  (where  $\dagger$  denotes the Moore-Penrose pseudo-inverse).  $\mathbf{x}_t$  can be recovered from  $\bar{\mathbf{x}}_t$ .  $\eta \in (0, 1]$  is a hyperparameter controlling the variance of the transitions, and  $\eta$  and  $\eta_b$  may depend on  $\sigma_t, s_i, \sigma_{\mathbf{y}}$ . Set a big enough  $\sigma_T$  that  $\sigma_T \geq \sigma_{\mathbf{y}}/s_i$  for all positive  $s_i$ "

Then, the authors of DDRM defined the model distribution:  $p_\theta$  as a series of Gaussian conditionals. Similar to DDPM, they obtain predictions of  $\mathbf{x}_0$  at every step  $t$ . Specifically, they defined DDRM with trainable parameters  $\theta$  as follows:

$$p_\theta^{(T)}(\bar{\mathbf{x}}_T^{(i)} | \mathbf{y}) = \begin{cases} \mathcal{N}\left(\bar{\mathbf{y}}^{(i)}, \sigma_T^2 - \frac{\sigma_{\mathbf{y}}^2}{s_i^2}\right) & \text{if } s_i > 0 \\ \mathcal{N}(0, \sigma_T^2) & \text{if } s_i = 0 \end{cases} \quad (8)$$

$$p_\theta^{(t)}(\bar{\mathbf{x}}_t^{(i)} | \mathbf{x}_{t+1}, \mathbf{y}) = \begin{cases} \mathcal{N}\left(\bar{\mathbf{x}}_{\theta,t}^{(i)} + \sqrt{1 - \eta^2} \sigma_t \frac{\bar{\mathbf{x}}_{t+1}^{(i)} - \bar{\mathbf{x}}_{\theta,t}^{(i)}}{\sigma_{t+1}}, \eta^2 \sigma_t^2\right) & \text{if } s_i = 0 \\ \mathcal{N}\left(\bar{\mathbf{x}}_{\theta,t}^{(i)} + \sqrt{1 - \eta^2} \sigma_t \frac{\bar{\mathbf{y}}^{(i)} - \bar{\mathbf{x}}_{\theta,t}^{(i)}}{\sigma_{\mathbf{y}}/s_i}, \eta^2 \sigma_t^2\right) & \text{if } \sigma_t < \frac{\sigma_{\mathbf{y}}}{s_i} \\ \mathcal{N}\left((1 - \eta_b) \bar{\mathbf{x}}_{\theta,t}^{(i)} + \eta_b \bar{\mathbf{y}}^{(i)}, \sigma_t^2 - \frac{\sigma_{\mathbf{y}}^2}{s_i^2} \eta_b^2\right) & \text{if } \sigma_t \geq \frac{\sigma_{\mathbf{y}}}{s_i} \end{cases}$$

$\mathbf{x}_{\theta,t}$  represents the prediction made by a model  $f_\theta(\mathbf{x}_{t+1}, t+1) : \mathbb{R}^n \times \mathbb{R} \rightarrow \mathbb{R}^n$  that takes in the sample  $\mathbf{x}_{t+1}$  and the conditioned time step  $(t+1)$ .  $\bar{\mathbf{x}}_{\theta,t}^{(i)}$  denotes  $i$ -th index of  $\bar{\mathbf{x}}_{\theta,t} = \mathbf{V}^\top \mathbf{x}_{\theta,t}$ .

Compared to  $q^{(t)}$ , the definition of  $p_\theta^{(t)}$  merely replaces  $\bar{\mathbf{x}}_0^{(i)}$  (which is unknown at sampling) with  $\bar{\mathbf{x}}_{\theta,t}^{(i)}$  (which depends on the predicted  $\mathbf{x}_{\theta,t}$ ) when  $t < T$ , and replaces  $\bar{\mathbf{x}}_0^{(i)}$  with 0 when  $t = T$ .

### 3.4 Pretrained models instead of Learning

As mentioned in the previous section, Eq.(8) will obtain predictions of  $\mathbf{x}_0$  at every step  $t$ . The prediction process is parameterized with  $\theta$ . After defining Eq.(7) and (8) by choosing  $\sigma_{1:T}, \eta$  and  $\eta_b$ , it is typical to learn  $\theta$  by maximizing ELBO2 mentioned in Subsection 3.2.2. However, for each inverse problem with a different  $\mathbf{H}$  and  $\sigma_{\mathbf{y}}$ , it is necessary to train a different model. The authors of DDRM proposed another way to use the pre-trained DDPM model to deal with arbitrary linear inverse problems.

Table 1: 4× super-resolution and Gaussian deblurring results on ImageNet 1K ( $256 \times 256$ ) without additive noise ( $\sigma_y = 0$ ). We compute the average PSNR (dB), average SSIM, and KID ( $\times 10^3$ ).

Method	4× super-resolution				Deblurring			
	PSNR↑	SSIM↑	KID↓	NFEs↓	PSNR↑	SSIM↑	KID↓	NFEs↓
Baseline	25.65	0.71	44.90	0	19.26	0.48	38.00	0
DGP	23.06	0.56	21.22	1500	22.70	0.52	27.60	1500
RED	<b>26.08</b>	<b>0.73</b>	53.55	100	26.16	0.76	21.21	500
SNIPS	17.58	0.22	35.17	1000	34.32	<b>0.87</b>	<b>0.49</b>	1000
DDRM	<b>26.55</b>	<b>0.72</b>	<b>7.22</b>	<b>20</b>	<b>35.64</b>	<b>0.95</b>	0.71	<b>20</b>
DDRM-OUR	24.29	0.67	<b>12.28</b>	<b>20</b>	<b>36.91</b>	<b>0.95</b>	<b>0.69</b>	<b>20</b>

Table 2: 4× super-resolution and Gaussian deblurring results on ImageNet 1K ( $256 \times 256$ ) with additive noise ( $\sigma_y = 0.05$ ). We compute the average PSNR (dB), average SSIM, and KID ( $\times 10^3$ ).

Method	4× super-resolution				Deblurring			
	PSNR↑	SSIM↑	KID↓	NFEs↓	PSNR↑	SSIM↑	KID↓	NFEs↓
Baseline	22.55	0.46	67.86	0	18.35	0.20	75.50	0
DGP	20.09	0.43	42.17	1500	21.20	0.45	34.02	1500
RED	22.90	0.49	43.45	100	14.69	0.08	121.82	500
SNIPS	16.30	0.14	67.77	1000	16.37	0.14	77.96	1000
DDRM	<b>25.21</b>	<b>0.66</b>	<b>12.43</b>	<b>20</b>	<b>25.45</b>	<b>0.66</b>	<b>15.24</b>	<b>20</b>
DDRM-OUR	<b>23.03</b>	<b>0.60</b>	<b>9.75</b>	<b>20</b>	<b>25.05</b>	<b>0.70</b>	<b>5.71</b>	<b>20</b>

The authors proved that if the settings of  $\eta$  and  $\eta_b$  fulfill some conditions and the prediction models  $f_\theta(\mathbf{x}_{t+1}, t+1)$  don't have weight sharing across time steps, ELBO2 of DDRM can be rewritten in the form of ELBO1 of DDPM. We refer interested readers to Appendix C of [1] for more details.

Therefore, it is possible to use pertained models of DDPM as the predicted models in the DDRM models of Eq.(8) to recover the signal. For different linear inverse problems, it is only necessary to modify  $\mathbf{H}$  and its SVD decomposition without training parameterized prediction models.

### 3.5 Our implemented way

We re-implemented DDRM models based on the previously mentioned method. Then, we performed deblur, super-resolution, and inpainting tasks using our implementation and compared the results with the original paper.

## 4 Data

We performed an evaluation on ImageNet 1K ( $256 \times 256$ ) [22] dataset and we randomly selected one image from each category, namely 1000 hold-out validation images to compute average peak signal-to-noise ratio (PSNR), average structural similarity index measure (SSIM), and kernel Inception distance (KID). We also chose several human face images from FFHQ  $256 \times 256$  [23] dataset for the demo test. As our reimplementations is training-free, we use pre-trained models from [24] and [25] to conduct experiments on the ImageNet and FFHQ, respectively.

## 5 Experiments and findings

Table 1 and 2 shows the results of quantitative experiments comparison when we apply the same parameter settings as the original DDRM. PSNR and SSIM reflect the faithfulness of the restoration image to the original image, and KID measures the quality of the generated image. When we apply the same neural function evaluations (NFEs), all three mentioned metrics can achieve the comparable or even better values as original DDRM. Due to the page limit, please check out our GitHub repository for more detailed contributions of our reimplementations.

We perform the experiments on noiseless images ( $\sigma_y = 0$ ) or images with additive white Gaussian noise ( $\sigma_y = 0.05$ ). The degradation models are specified as follows: (i) For super-resolution,

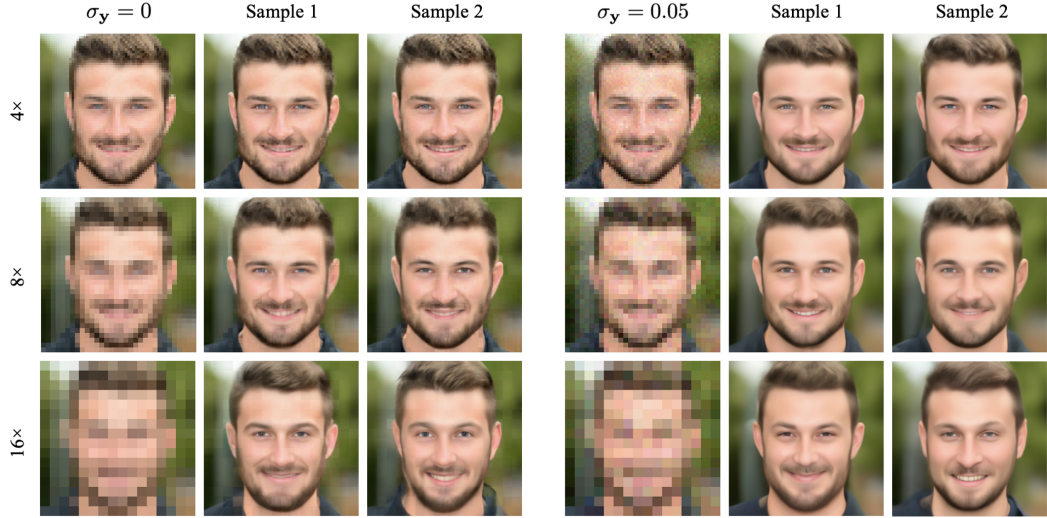


Figure 2: Super-resolution restoration results.

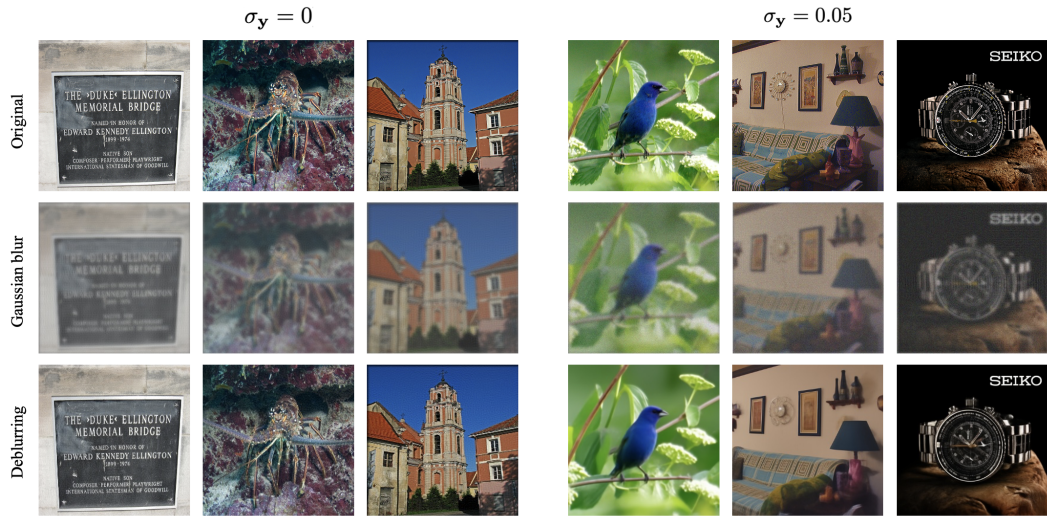


Figure 3: Deblurring results on ImageNet images.

we downscale the images by  $4\times$ ,  $8\times$ , and  $16\times$  via a block averaging filter. Figure 2 shows the measurements with lower resolution and their restoration samples. (ii) For deblurring, we implement the gaussian blur with a kernel of size  $5\times 5$  and a standard deviation of 10.0. Figure 3 displays the images with Gaussian deblur degradation and corresponding restoration results. (ii) For inpainting, we mask parts of the original image with a square block, text overlay, and random missing with rate 50% of the pixels. The inpainting restoration effect is remarkable in Figure 4 taking advantage of the DDPM pre-trained on FFHQ [25].

## 6 Challenges

The DDRM paper provided a comprehensive overview of the methodology and results, with sufficient additional information in the appendices to allow us to re-implement it efficiently. We did, however, encounter some challenges in debugging the process. For example, making sure we do the correct



Figure 4: Inpainting results on FFHQ face images.

operations in parts of the code was very important. In some instances, our tensors were correctly sized, albeit having applied the wrong transformations. Consequently, our estimated image was inconsistent. Thus, we had a compelling reason to holistically understand the DDRM method, so we can apply it from a logical perspective and not only rely on the programmatic context.

We did not directly contact the authors, but we did look at some parts of their code. Specifically, we borrowed some utility functions from them, namely, SVD utilities, the inpainting masks, and some other general-purpose utility functions they used.

## 7 Ethical consideration, societal impact, alignment with UN SDG targets

While generative models have the potential to revolutionize areas in healthcare and education, they also pose significant risks. One of the primary concerns is their misuse for creating fake content or spreading misinformation. [26]

Another concern is the weaponization of DDRM to spread false information. [27] The ease of access and use of these models can lead to an increase in the quantity and quality of misinformation. [28] This situation raises multiple ethical and human rights concerns. [26] However, then the question becomes whether the technology itself is evil or the party that is using it is, and it pulls into question the responsibility of the authors to provide appropriate counter-measures, as discussed in [29].

Moreover, the design of current generative AI could make it hard to alter people’s perceptions once exposed to false information. [30] Therefore, while DDRM and similar technologies hold great promise, it is crucial to implement safeguards to prevent their misuse, as discussed by the scientists at OpenAI in [31]. Additionally, they can also inadvertently perpetuate biases present in the training data, for example the gender bias as described in [32]. Cultural insensitivity, gender bias, racial stereotypes, and other forms of prejudice can all manifest in generated content. [33]

DDRM’s potential applications in healthcare, education, and content creation align with several SDGs, including SDG 3 (Good Health and Well-being) [34], SDG 4 (Quality Education) [35], and SDG 17 (Partnerships for the Goals) [36].

Generative models could be used to enhance healthcare applications, such as image analysis for medical diagnosis. In [37], the authors discuss the use of digital technology to improve healthcare. By applying DDRM in specific situations on medical images, doctors could identify previously unnoticed singularities in patient data, thereby directly impacting SDG 3 [34].

Additionally, by proving the re-implementation of DDRM is possible, we are fostering collaboration and open-source development of generative models. This could promote responsible innovation and encourage the community to pay more attention in making their work reproducible. Consequently, our re-implementation indirectly pushes SDG 9 (Industry, Innovation, and Infrastructure) [38] and SDG 17 [36].

## 8 Conclusion

In this work, we study and reimplement DDRM. After that, we perform experiments using our implementation on FFHQ and ImageNet dataset. We analyze the performance metrics PSN, SSIM, and KID and find that the results of our implementation are very close to the ones of the original paper.

## 9 Self-assessment

We think that our project should be graded with a B mainly for the following reasons

- We have produced a structured and overall successful reproduction. It is non-trivial of the implemented structure that embeds other pre-trained models to provide information in the generative model.
- Besides one original dataset, on a new dataset, we also compared not only our implementation and the original paper but also other methods. We show the reproducibility of the original paper by the additional comparison experiments.
- We used two different weights of the pre-trained DDPM from the ones used in the original paper. The experiments are novel to show that DDRM can work and reach similar performance under different embedded pre-trained models. We believe our paper fulfills one criterion of Excellent Project (B-A): novel, interesting, and informative new metrics and/or ways of evaluating the methods.

## References

- [1] Bahjat Kawar, Michael Elad, Stefano Ermon, and Jiaming Song. Denoising diffusion restoration models, 2022.
- [2] Xingang Pan, Xiaohang Zhan, Bo Dai, Dahua Lin, Chen Change Loy, and Ping Luo. Exploiting deep generative prior for versatile image restoration and manipulation, 2020.
- [3] Bahjat Kawar, Gregory Vaksman, and Michael Elad. Snips: Solving noisy inverse problems stochastically. *Advances in Neural Information Processing Systems*, 34:21757–21769, 2021.
- [4] Yaniv Romano, Michael Elad, and Peyman Milanfar. The little engine that could: Regularization by denoising (red). *SIAM Journal on Imaging Sciences*, 10(4):1804–1844, 2017.
- [5] Maitreya Suin, Kuldeep Purohit, and AN Rajagopalan. Image restoration using feature-guidance. *arXiv preprint arXiv:2201.00187*, 2022.
- [6] Syed Waqas Zamir, Aditya Arora, Salman Khan, Munawar Hayat, Fahad Shahbaz Khan, Ming-Hsuan Yang, and Ling Shao. Learning enriched features for fast image restoration and enhancement. *IEEE Transactions on Pattern Analysis and Machine Intelligence*, 45(2):1934–1948, 2023.
- [7] Yuelong Li, Mohammad Tofighi, Junyi Geng, Vishal Monga, and Yonina C Eldar. Efficient and interpretable deep blind image deblurring via algorithm unrolling. *IEEE Transactions on Computational Imaging*, 6:666–681, 2020.
- [8] Zheng Chen, Yulun Zhang, Ding Liu, Bin Xia, Jinjin Gu, Linghe Kong, and Xin Yuan. Hierarchical integration diffusion model for realistic image deblurring. *arXiv preprint arXiv:2305.12966*, 2023.
- [9] Muhammad Asim, Fahad Shamshad, and Ali Ahmed. Blind image deconvolution using deep generative priors, 2019.
- [10] Dmitry Ulyanov, Andrea Vedaldi, and Victor Lempitsky. Deep image prior. *International Journal of Computer Vision*, 128(7):1867–1888, March 2020.

- [11] Meiya Chen, Yi Chang, Shuning Cao, and Luxin Yan. Learning blind denoising network for noisy image deblurring. In *ICASSP 2020 - 2020 IEEE International Conference on Acoustics, Speech and Signal Processing (ICASSP)*, pages 2533–2537, 2020.
- [12] Yichun Jiang, Yunqing Liu, Weida Zhan, and Depeng Zhu. Improved thermal infrared image super-resolution reconstruction method base on multimodal sensor fusion. *Entropy*, 25(6):914, 2023.
- [13] Jie Liang, Hui Zeng, and Lei Zhang. Details or artifacts: A locally discriminative learning approach to realistic image super-resolution, 2022.
- [14] Hamdollah Nasrollahi, Kamran Farajzadeh, Vahid Hosseini, Esmaeil Zarezadeh, and Milad Abdollahzadeh. Deep artifact-free residual network for single-image super-resolution. *Signal, Image and Video Processing*, 14(2):407–415, October 2019.
- [15] Hengyuan Ma, Li Zhang, Xiatian Zhu, Jingfeng Zhang, and Jianfeng Feng. Accelerating score-based generative models for high-resolution image synthesis, 2022.
- [16] Christian Ledig, Lucas Theis, Ferenc Huszar, Jose Caballero, Andrew Cunningham, Alejandro Acosta, Andrew Aitken, Alykhan Tejani, Johannes Totz, Zehan Wang, and Wenzhe Shi. Photo-realistic single image super-resolution using a generative adversarial network, 2017.
- [17] Bee Lim, Sanghyun Son, Heewon Kim, Seungjun Nah, and Kyoung Mu Lee. Enhanced deep residual networks for single image super-resolution, 2017.
- [18] Riya Shah, Anjali Gautam, and Satish Kumar Singh. Overview of image inpainting techniques: A survey. In *2022 IEEE Region 10 Symposium (TENSYMP)*, pages 1–6, 2022.
- [19] Deepak Pathak, Philipp Krahenbuhl, Jeff Donahue, Trevor Darrell, and Alexei A. Efros. Context encoders: Feature learning by inpainting, 2016.
- [20] Jiahui Yu, Zhe Lin, Jimei Yang, Xiaohui Shen, Xin Lu, and Thomas S. Huang. Generative image inpainting with contextual attention, 2018.
- [21] Jascha Sohl-Dickstein, Eric A. Weiss, Niru Maheswaranathan, and Surya Ganguli. Deep unsupervised learning using nonequilibrium thermodynamics, 2015.
- [22] Olga Russakovsky, Jia Deng, Hao Su, Jonathan Krause, Sanjeev Satheesh, Sean Ma, Zhiheng Huang, Andrej Karpathy, Aditya Khosla, Michael Bernstein, et al. Imagenet large scale visual recognition challenge. *International journal of computer vision*, 115:211–252, 2015.
- [23] Tero Karras, Samuli Laine, and Timo Aila. A style-based generator architecture for generative adversarial networks. In *Proceedings of the IEEE/CVF conference on computer vision and pattern recognition*, pages 4401–4410, 2019.
- [24] Prafulla Dhariwal and Alexander Nichol. Diffusion models beat gans on image synthesis. *Advances in neural information processing systems*, 34:8780–8794, 2021.
- [25] Jooyoung Choi, Sungwon Kim, Yonghyun Jeong, Youngjune Gwon, and Sungroh Yoon. Ilvr: Conditioning method for denoising diffusion probabilistic models. *arXiv preprint arXiv:2108.02938*, 2021.
- [26] Noémi Bontridder and Yves Poulet. The role of artificial intelligence in disinformation. *Data Policy*, 3:e32, 2021.
- [27] Veena McCoole and Elan Kane. Safeguarding Generative AI Models from Spreading Misinformation with Transparently Sourced Data - NewsGuard — newsguardtech.com. <https://www.newsguardtech.com/insights/>, May 2023. [Accessed 15-12-2023].
- [28] Felix M Simon, Sacha Altay, and Hugo Mercier. Misinformation reloaded? fears about the impact of generative ai on misinformation are overblown. *Harvard Kennedy School Misinformation Review*, 4(5), 2023.

- [29] Christoph Trattner, Dietmar Jannach, Enrico Motta, Irene Costera Meijer, Nicholas Diakopoulos, Mehdi Elahi, Andreas L Opdahl, Bjørnar Tessem, Njål Borch, Morten Fjeld, et al. Responsible media technology and ai: challenges and research directions. *AI and Ethics*, 2(4):585–594, 2022.
- [30] Celeste Kidd and Abeba Birhane. How ai can distort human beliefs. *Science*, 380(6651):1222–1223, 2023.
- [31] Josh A. Goldstein, Girish Sastry, Micah Musser, Renee DiResta, Matthew Gentzel, and Katerina Sedova. Generative language models and automated influence operations: Emerging threats and potential mitigations, 2023.
- [32] Ashley Hua, Nicholas Lu, Mingchuan Cheng, Andrew Wang, and Jason Minghan Dong. Automatic gender bias detection in digital content. *International Journal of Computational and Biological Intelligent Systems*, 4(1), 2022.
- [33] Leonardo Nicoletti and Dina Bass. Humans Are Biased. Generative AI Is Even Worse — bloomberg.com. <https://www.bloomberg.com/graphics/2023-generative-ai-bias/>. [Accessed 15-12-2023].
- [34] Rosa Maria Fernandez. *SDG3 Good Health and Well-Being: Integration and Connection with Other SDGs*, pages 629–636. Springer International Publishing, Cham, 2020.
- [35] Munish Saini, Eshan Sengupta, Madanjit Singh, Harnoor Singh, and Jaswinder Singh. Sustainable development goal for quality education (sdg 4): A study on sdg 4 to extract the pattern of association among the indicators of sdg 4 employing a genetic algorithm. *Education and Information Technologies*, 28(2):2031–2069, Feb 2023.
- [36] Isabel B. Franco and Masato Abe. *SDG 17 Partnerships for the Goals*, pages 275–293. Springer Singapore, Singapore, 2020.
- [37] Naresh Kasoju, NS Remya, Renjith Sasi, S Sujesh, Biju Soman, C Kesavadas, CV Muraleedharan, PR Harikrishna Varma, and Sanjay Behari. Digital health: trends, opportunities and challenges in medical devices, pharma and bio-technology. *CSI Transactions on ICT*, pages 1–20, 2023.
- [38] UN ESCAP et al. Sdg 9: Industry, innovation and infrastructure. 2023.